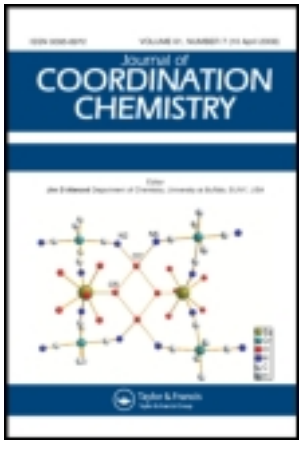

Journal of Coordination Chemistry
Publication details, including instructions for authors and subscription information:
http://www.tandfonline.com/loi/gcoo20

Reactivities of coordinated phosphodiesters

R.D. Wijesekera [a] & A.M. Sargeson [b]
[a] University of Colombo, PO Box 1490, Colombo 3, Sri Lanka
[b] Research School of Chemistry, Australian National University, Canberra, A.C.T. 0200, Australia
Published online: 25 Jan 2007.

To cite this article: R.D. Wijesekera & A.M. Sargeson (2005): Reactivities of coordinated phosphodiesters, Journal of Coordination Chemistry, 58:1, 3-19

To link to this article: http://dx.doi.org/10.1080/00958970512331327393

Journal of Coordination Chemistry
Vol. 58, No. 1, 10 January 2005, 3–19

Reactivities of coordinated phosphodiesters*

R.D. WIJESEKERA‡ and A.M. SARGESON†§

‡University of Colombo, PO Box 1490, Colombo 3, Sri Lanka
§Research School of Chemistry, Australian National University, Canberra, A.C.T. 0200, Australia

(Received 7 September 2004; revised 4 October 2004; in final form 19 October 2004)

The amminolysis and hydrolysis of the ester moieties in $[(NH_3)_5Co(bnpp)]^{2+}$ and *cis*-$[(en)_2Co(OH)(bnpp)]^{+}$ (where bnpp = bis(4-nitrophenylphosphate) and en = 1,2-ethanediamine) in aqueous solution at 25°C have been followed over a range in pH. In each instance, cleavage of 4-nitrophenol occurred in two observable events triggered by the coordinated nucleophiles, amido ion and hydroxo ion. The mechanistic pathways have been analyzed and the rate enhancements evaluated relative to uncoordinated substrates and other relevant literature data. The analysis indicates requirements for the metal reagent to be effective in phosphate ester hydrolysis and phosphoryl transfer.

Keywords: Metal ion activated phosphate ester cleavage; Cobalt; Phosphate ester; Phosphoryl transfer

1. Introduction

Enzymic hydrolysis of P–O bonds in phosphate derivatives occurs many orders of magnitude faster than the uncatalyzed reactions and numerous studies have been conducted in attempts to understand the origins of the extraordinary reactivity, especially of the metal ion-catalyzed enzymic processes. Proposals based on the presence of metal-bound nucleophiles and induction of strain due to the formation of four-membered chelates have been advanced to account for the rapid hydrolysis rates [1–3]. A precedent for the latter is provided by hydrolytic studies of organic phosphates where cyclic five-membered esters were shown to hydrolyze up to 10^7 times faster than their acyclic analogs [4,5]. This was attributed to the presence of a strained ring system, which lowered the activation energy of the cyclic ester relative to that of the acyclic species.

†Corresponding author. E-mail: sargeson@rsc.anu.edu.au
*In memory of Arthur Martell, a sterling champion of coordination chemistry

Journal of Coordination Chemistry
ISSN 0095-8972 print: ISSN 1029-0389 online
DOI: 10.1080/00958970512331327393

In order to evaluate these proposals, studies have been conducted with two broad classes of model compounds, comprising complexes that react primarily via intramolecular attack of a coordinated amido ion at the phosphorus center [6–9] generated by deprotonation of a *cis* ammonia in molecules such as [(npp)pentaamminecobalt(III)]$^{+}$, [(dnpp)pentaamminecobalt(III)]$^{+}$, [fluorophosphatopentaamminecobalt(III)]$^{+}$, [$(NH_3)_5$Co(enpp)]$^{2+}$, [$(NH_3)_5$Ir(bnpp)]$^{2+}$ and [$(NH_3)_5$Ir(enpp)]$^{2+}$ and those in which the *cis* nucleophile is a metal-bound hydroxide ion [2,9] derived from deprotonation of ions such as *cis*[$(en)_2$Co(OH_2)(npp)]$^{+}$, *cis*[$(en)_2$Ir(OH_2)(enpp)]$^{2+}$ and *cis*[$(en)_2$Ir(OH_2)(bnpp)]$^{2+}$ (where npp = 4-nitrophenylphosphate, dnpp = 2,4-dinitrophenylphosphate, enpp = ethyl-4-nitrophenylphosphate, bnpp = bis(4-nitrophenyl)phosphate and en = 1,2-ethanediamine). With the former class of compounds, intramolecular attack of the coordinated amido ion at the phosphorus center generates the aminophosphorane intermediate, which then decays to the chelate phosphoramidate or chelate phosphoramidate ester. Although chelate phosphoramidate intermediates were observed for two of the systems ([$(NH_3)_5$Co(dnpp)]$^{+}$ and [$(NH_3)_5$Co(enpp)]$^{2+}$), the chelated species then ring opened via Co–O bond rupture without exocyclic hydrolysis of the ester group. The behavior of the more inert Ir(III) complexes was explored to try to limit the metal–ligand bond rupture and induce exocyclic ester cleavage. However, hydrolysis of the diesters in [$(NH_3)_5$Ir(enpp)]$^{2+}$ and [$(NH_3)_5$Ir(bnpp)]$^{2+}$ also yielded the ring-opened monoester species. Nevertheless, in part, the expectation of reactivity for the cyclic monoester complex was met because the ring-opening reaction occurred at the P–O bond and not at the Ir–O bond. If the Ir–O group is regarded as an ester equivalent, this implicitly reflects enhanced reactivity at the strained 4-chelate ring but of an endocyclic nature in preference to exocyclic ester hydrolysis. A complex that generates a cyclic intermediate with a better leaving group in a less strained ring system than that of the Ir(III) chelate may therefore induce some exocyclic cleavage at the phosphorus center by a similar mechanism. For this reason, [$(NH_3)_5$Co(bnpp)]$^{2+}$ was synthesized and its reactivity was explored.

An alternative strategy involved intramolecular attack of coordinated OH^{-} at the phosphorus center of coordinated phosphate diesters, specifically *cis*[$(en)_2$Ir(OH)(enpp)]$^{+}$ and *cis*[$(en)_2$Ir(OH)(bnpp)]$^{+}$. The chelate monoester was not observed in either case. The observed product was a monodentate monoester species, formed via rapid P–O bond rupture of the strained chelate monoester intermediate. It was anticipated that the strained four-membered ring would be less strained and might be observable if the smaller Co(III) replaced the Ir(III) ion. For this reason, *cis*[$(en)_2$Co(OH_2)(bnpp)]$^{2+}$ was synthesized and its reactivity explored.

Another reason for investigating this system was to clarify somewhat contradictory results arising from other studies on metal ion-promoted hydrolyses of phosphate esters. Specifically, *cis*[$(en)_2$Ir(OH_2)(bnpp)]$^{2+}$ hydrolyzes more rapidly [9] than the corresponding monoester complex *cis*[$(en)_2$Ir(OH_2)(npp)]$^{+}$. However, *cis*[(N_4)Co(OH)(OH_2)]$^{2+}$ [N_4 = $(en)_2$ and trpn (= tris(3-amino-propyl)amine), respectively] promoted rates of hydrolysis of the diesters bnpp [10] and bdnpp (= bis(2,4-dinitrophenyl) phosphate) [11] were less (5–10-fold) than those of the corresponding monoesters. The conflicting differences in reactivity of the phosphate esters is surprising as similarly reactive species are expected to be involved. Direct comparison of the hydrolytic behavior of bnpp and npp in the *cis*[$(en)_2$Co(OH)(bnpp)]$^{+}$, *cis*[$(en)_2$Co(OH)(npp)], *cis*[$(en)_2$Co(OH)(OH_2)]$^{2+}$/bnpp and *cis*[$(en)_2$Co(OH)(OH_2)]$^{2+}$/npp systems would

help to identify the features that govern the variation in rates and mechanisms of these reactions.

2. Experimental

Analytical grade reagents were used unless stated otherwise. ^{31}P NMR spectra were recorded with a Varian VXR-300 spectrometer at 121.42 MHz. Chemical shifts were obtained in ppm relative to 85% H_3PO_4 as an external standard. Triethylphosphate was used as the internal standard. ^{1}H NMR spectra were recorded with a Gemini-300 spectrometer at 300.1 MHz with NaTPS as the internal standard. Chemical shifts (δ positive downfield) are given relative to this standard in ppm. Electronic spectra and kinetic traces were obtained with a Hewlett Packard HP 8450A diode array spectrophotometer fitted with a thermostatted cell holder, a Cary 118C spectrophotometer fitted with a recirculating water bath or an Applied Photophysics model SF.17MV stopped flow spectrophotometer. H^+ measurements were carried out with a Radiometer PHM 26 pH meter calibrated using standard buffers and G202C glass and K4122 calomel electrodes. All evaporations were carried out on a rotary evaporator at ~20 Torr such that the solution temperature did not exceed 25°C.

$[(NH_3)_5Co(CF_3SO_3)](CF_3SO_3)_2$ [12–14], $[(NH_3)_5Co(npp)](ClO_4)$ [6], *cis*$[(en)_2Co(CF_3SO_3)_2](CF_3SO_3)$ [12–14] and *cis*$[(en)_2Co(OH_2)(npp)](ClO_4)$ [2] were synthesized as described in the references.

2.1 *[(NH₃)₅Co(OP(O)(OC₆H₄NO₂)₂)](CF₃SO₃)₂([(NH₃)₅Co(bnpp)](CF₃SO₃)₂)*

$HOP(O)(OC_6H_4NO_2)_2$ (0.64 g) and 2,4,6-collidine (0.25 mL) were added to dry sulfolane (15 mL) and the solution warmed to ~45°C. When the bnpp had dissolved, $[(NH_3)_5Co(CF_3SO_3)](CF_3SO_3)_2$ (1 g) was added and heating continued for 5 h. The solution was then cooled to 25°C and washed repeatedly with ether. The solid residue thus obtained was dissolved in a minimum volume of acetone (10 mL), and the acetone solution added slowly, with stirring, to H_2O (2 L, acidified to pH 2 with HCl). The solution developed some cloudiness, which persisted even on dilution. After absorption on a Sephadex SP-C25 column (Na^+ form) previously equilibrated with water (pH 2), the product was eluted as the second band with 0.15 M NaCl (pH 2/HCl). This fraction was evaporated to 25 mL and kept at 0°C for 2–3 h. The pink crystals formed were collected and dissolved in a minimum volume of water (pH ~2). Sodium triflate was added to the ice-cold solution and the crystals that formed were filtered off, washed with ethanol and ether and dried under vacuum over P_2O_5. (Yield 53%.) Anal. Calcd. for $C_{14}H_{23}N_7CoF_6O_{14}PS_2$(%): C, 21.52; H, 2.97; N, 12.55; Co, 7.15; P, 3.96; S, 8.21. Found: C, 21.3; H, 3.2; N, 12.2; Co, 7.2; P, 4.3; S, 7.9. ^{1}H NMR (D_2O): 8.3 (d) $J_{H-H} = 9$ Hz (4H); 7.3 (d) $J_{H-H} = 9$ Hz (4H); 4.2 (br) (12H). *cis* NH_3 was probably obscured by HOD peak (4.9). $^{31}P\{^{1}H\}$ NMR (pH 8.8): −6.4 (s). Electronic spectrum $(\lambda, \varepsilon)_{max}$: 518 nm, 132 $M^{-1}\,cm^{-1}$; 320, 4.72×10^4; 242, 4.89×10^4.

2.2 *cis[(en)₂Co(OH₂)(OP(O)(OC₆H₄NO₂)₂)]S₂O₆·H₂O (cis[(en)₂ Co(OH₂)(bnpp)]S₂O₆·H₂O)*

$HOP(O)(OC_6H_4NO_2)_2$ (1 g) was dissolved in dry sulfolane (20 mL) with the addition of 2,4,6-collidine (0.35 mL). *cis*$[(en)_2Co(CF_3SO_3)_2](CF_3SO_3)$ (1.84 g) was added and the

resulting solution heated at 50°C for 5 h. The solution was cooled, repeatedly washed with ether and the solid residue thus obtained dissolved in a minimum volume of acetone (15 mL). This acetone solution was added slowly, with stirring, to water (2 L) acidified to pH 2 with HCl. On addition of the acetone solution to water a cloudiness resulted that persisted even on dilution. The aqueous solution was then sorbed on a Sephadex SP-C25 column (Na^+ form) previously equilibrated with water (pH 2) and the product eluted with 0.2 M NaCl (pH 2). The desired product was contained in the second band off the column and was evaporated to 50 mL and cooled at 4°C for 3–4 h. The pink crystals that formed were collected, dissolved in a minimum volume of water (pH 2) and the product reprecipitated as the dithionate salt on addition of $Li_2S_2O_6$. The crystals were collected and dried under vacuum over P_2O_5. (Yield 68%.) Anal. Calcd. for $C_{16}H_{28}N_6CoO_2PS_2$(%): C, 26.90; H, 3.95; N, 11.76; Co, 8.25; P, 4.34; S, 8.97. Found: C, 27.0; H, 3.8; N, 11.6; Co, 8.4; P, 4.2; S, 8.3. ^{1}H NMR spectrum (pH 3): 8.3 (d) $J_{H-H} = 9$ Hz (4H); 7.3 (d) $J_{H-H} = 9$ Hz (4H); 6.9–5.9 (8H); 2.9 (br) (4H); 2.6 (br) (4H). $^{31}P\{^1H\}$ NMR spectrum (pH 3.5): −5.7 (s). Electronic spectrum $(\lambda, \varepsilon)_{max}$: 502, 121 $M^{-1}\,cm^{-1}$; 305, 1.1×10^4.

2.3 *Kinetics and further experiments*

2.3.1 $[(NH_3)_5Co(OP(O)(OC_6H_4NO_2)_2)](CF_3SO_3)_2$. The initial step in the hydrolysis was followed spectrophotometrically at 400 nm by monitoring the release of 4-nitrophenolate ion over five half-lives at 25°C. The reaction was initiated either by: (i) adding 10 μL of a stock solution (prepared by dissolving 3–5 mg of complex in 1 mL H_2O acidified to pH 3) to a series of 1 M buffer/hydroxide solutions maintained at $I = 1.0$ M (NaCl); (ii) mixing equal volumes of solutions of twice the desired concentration of the complex and buffer in a stopped flow apparatus (buffer abbreviations: CAPS, 3-(cyclohexylamino)propane sulfonic acid; CHES, 2-(cyclohexylamino)ethane sulfonic acid; HEPES, *N*-2-hydroxyethylpiperazinyl-*N*′-ethane sulfonic acid; MES, 2-(*N*-morpholino)ethane sulfonic acid; PIPES, piperazindiyl-*N*,*N*′-bis(2-ethane sulfonic acid; TRIS, tris(hydroxymethyl)amino ethane). The ionic strength of the solution was maintained at 1.0 M (NaCl). The pH of the reaction mixture was measured after the reaction.

In order to follow the second step, cooled solutions of complex (3 mg in 1 mL H_2O) and NaOH (0.5 mL, 1 M) were reacted at 0°C for 5–6 s, quenched with 1 M HCl (0.25 mL) and the solution diluted to 50 mL with water (pH ~3). Aliquots of the solution were mixed with an equal volume of buffer/hydroxide solution of twice the desired concentration in a stopped flow apparatus and the reaction monitored at 400 nm, 25°C over five half-lives. The ionic strength of the solution was maintained at 1.0 M (NaCl) and the pH of the reaction mixture was measured after the reaction.

The rate constants for the two steps were sufficiently different to allow the reactions to be treated independently. The data followed a single exponential decay in each instance and were processed via the least-squares curve-fitting program LSTSQR or by a nonlinear regression method (Marquardt algorithm) [15]. The yield of nitrophenolate ion was determined from the final absorbance of the reaction mixture using a molar absorption coefficient of 18 700 $M^{-1}\,cm^{-1}$ at 400 nm.

The hydrolysis of the chloride salt was also followed by ^{31}P NMR spectroscopy at 25°C (acquisition frequency 121.42 MHz, spectral width 20 KHz, data points 16 384,

pulse angle 90°, pulse repetition time 0.7 s). The complex was generated, *in situ*, by stirring a suspension of the triflate salt (0.025 M) with Dowex AG1-X8 (Cl^- form) anion exchange resin in buffer/hydroxide solution at the desired pH. The ionic strength of these solutions was maintained at 1.0 M (NaCl).

The chloride salt (0.025 M), generated as described above, was reacted with: (i) 1 M CAPS buffer containing 20% D_2O at pH 10.5 ($\mu = 1.0$ M, NaCl) and 25°C, and an integrated ^{31}P NMR spectrum of the reaction mixture was recorded. The solution was cooled to 5°C and aliquots of NaOH (at 5°C) added. Integrated ^{31}P NMR spectra of the resulting solutions were recorded rapidly at 5°C. (ii) 1 M CHES buffer at pH 9.5. (iii) 0.2 M NaOH at 25°C.

Reaction mixtures (ii) and (iii) contained 20% D_2O, and were maintained at $\mu = 1.0$ M (NaCl). Integrated ^{31}P NMR spectra were recorded at 25°C after 1 h and 5 min, respectively. Authentic $[(NH_3)_5Co(npp)]^+$ was also added to these solutions and integrated ^{31}P NMR spectra recorded at 25°C.

A solution of NaOH at 5°C was added to a cooled solution of the chloride salt of the complex (generated as described above). The reaction was allowed to proceed for 5–6 s, then quenched with HCl and a ^{31}P NMR spectrum of the resulting solution was recorded rapidly at 5°C.

2.3.2 *cis*$[(en)_2Co(OH_2)(OP(O)(OC_6H_4NO_2)_2)]S_2O_6 \cdot H_2O$. The kinetics of the hydrolysis were followed spectrophotometrically at 400 nm by observing the release of nitrophenolate ion. Typically, 10 μL of a stock solution (prepared by dissolving 5 mg of the complex in 5 mL H_2O) was added to 1 M buffer/hydroxide solution (2 mL) at 25°C and the change in absorbance at 400 nm monitored over five half-lives. The ionic strength of the buffer/hydroxide solutions was maintained at 1.0 M with NaCl. The buffer dependence of the reaction rate was investigated by adding the stock solution (10 μL) to 0.5 M buffers (2 mL) at 25°C, $I = 1.0$ M (NaCl), and following the change in absorbance at 400 nm over five half-lives.

Faster reactions were followed with a stopped flow spectrophotometer. A solution of the complex (5–10 mg dissolved in 100 mL H_2O) was mixed with an equal volume of buffer/hydroxide solution of twice the desired concentration and the change in absorbance at 400 nm monitored over five half-lives at 25°C. The ionic strength of the solution was maintained at 1.0 M with NaCl. The pH of the reaction mixture was measured on completion.

Hydrolysis of the complex occurred via two consecutive steps with sufficiently different rates that they could be considered independently. The data for the faster reaction were fitted by a nonlinear regression method (Marquardt algorithm) [15] and those of the slower reaction processed via the least-squares curve-fitting program LSTSQR. The data fitted single exponential decays.

Hydrolysis was also followed by ^{31}P NMR spectroscopy at 25°C. The chloride salt of the complex was used to obtain suitable concentrations, generated by stirring a suspension of the dithionate salt (0.025 M) and Dowex AG1-X8 (Cl^- form) resin in the appropriate buffer. The hydrolysis was carried out in 1 M acetate (pH 5.20), MES (pH 6.30), HEPES (pH 7.10), TRIS (pH 8.30), CHES (pH 9.10) buffers and in 0.1 M NaOH solution containing 20% D_2O and an internal standard (triethylphosphate) maintained at $I = 1$ M with NaCl. *cis*$[(en)_2Co(OH_2)(npp)](ClO_4)$ was then added to the reaction mixture at pH 5.20 as an identity check.

3. Results

3.1 *[(NH$_3$)$_5$Co(OP(O)(OC$_6$H$_4$NO$_2$)$_2$)](CF$_3$SO$_3$)$_2$*

[(NH$_3$)$_5$Co(bnpp)]$^{2+}$, synthesized by reacting [(NH$_3$)$_5$Co(CF$_3$SO$_3$)](CF$_3$SO$_3$)$_2$ and bnpp$^-$ in sulfolane, was purified and then characterized by elemental analysis, ^{1}H NMR, ^{31}P NMR and UV/vis spectroscopy. The ^{31}P NMR spectrum of the complex showed the expected downfield shift of ~6 ppm, relative to that of the free ligand [16–20].

Hydrolysis of the complex in the pH range 5–14 was followed spectrophotometrically at 400 nm and 25°C. The reaction proceeded in two steps, each involving release of nitrophenolate ion. At pH > 12, however, the second step was significantly slower and the reactions could be analyzed independently. The yield of nitrophenolate ion was 67 ± 1% and 65 ± 1%, respectively, for the two stages. The pseudo first-order rate constants for the loss of the first nitrophenolate group are given in table 1. This reaction obeys the rate law, $v = k_1[[(NH_3)_5Co(bnpp)]^{2+}][OH^-]$, with a second-order rate constant $k_1 = 10.2\,dm^3\,mol^{-1}\,s^{-1}$ at 25°C.

Below pH 12, the second nitrophenolate ion releasing step was much faster than the first (e.g. at pH 10.5, the rate constants for the first and second steps were $2.7 \times 10^{-3}\,s^{-1}$ and $0.10\,s^{-1}$, respectively). In addition, more than one mole of nitrophenol was released per mole of total reactant (table 2).

In order to follow the kinetics of the second nitrophenol releasing step at the lower pH values, the intermediate had to be generated rapidly and then its hydrolysis

Table 1. Variation of rate constant with pH for the loss of the initial nitrophenolate group from [(NH$_3$)$_5$Co(bnpp)]$^{2+}$.*

pH	[OH$^-$] M	Buffer	$k_{obs} \times 10^{-2}$ (s^{-1})
9.00	–	CHES	0.0110 (±0.0003)
9.56	–	CHES	0.030 (±0.001)
9.90	–	CHES	0.069 (±0.003)
10.54	–	CAPS	0.270 (±0.008)
10.80	–	CAPS	0.44 (±0.02)
11.10	–	CAPS	0.85 (±0.03)
–	0.05	–	53 (±2)
–	0.10	–	115 (±5)
–	0.25	–	295 (±16)
–	0.50	–	635 (±20)
–	0.75	–	1004 (±30)
–	1.00	–	1280 (±50)

*Determined spectrophotometrically at 400 nm, $T = 25°C$, $I = 1.0$ M (NaCl).

Table 2. pH *vs.* nitrophenolate liberated on hydrolysis of [(NH$_3$)$_5$Co(bnpp)]$^{2+}$ at 25°C.

pH	Buffer	% Nitrophenolate
8.71	CHES	118 (±1)
9.56	CHES	119 (±1)
10.14	CHES	122 (±1)
10.80	CAPS	131 (±1)
11.10	CAPS	124 (±1)
11.58	CAPS	125 (±1)

Table 3. Rate constant *vs.* pH for the loss of the second nitrophenolate group from $[(NH_3)_5Co(bnpp)]^{2+}$.*

pH	$[OH^-]$ M	Buffer	k_{obs} (s^{-1})
5.30	–	Acetate	0.30 (±0.01)
5.78	–	MES	0.37 (±0.01)
6.20	–	MES	0.65 (±0.02)
6.78	–	MES	1.03 (±0.03)
6.86	–	MES	1.08 (±0.03)
7.26	–	HEPES	1.28 (±0.04)
7.79	–	HEPES	1.34 (±0.04)
8.39	–	CHES	1.26 (±0.04)
8.93	–	CHES	1.10 (±0.03)
9.47	–	CHES	0.66 (±0.02)
10.05	–	CAPS	0.27 (±0.01)
10.57	–	CAPS	0.101 (±0.003)
10.83	–	CAPS	0.049 (±0.001)
–	0.01	–	0.035 (±0.001)
–	0.05	–	0.029 (±0.001)
–	0.10	–	0.028 (±0.001)
–	0.25	–	0.029 (±0.001)
–	0.50	–	0.028 (±0.001)
–	0.75	–	0.027 (±0.001)
–	1.00	–	0.030 (±0.001)

*Determined spectrophotometrically at 400 nm, $T = 25°C$, $I = 1.0$ M (NaCl).

monitored at 400 nm, 25°C. The pH rate constant profile of the intermediate consisted of a bell-shaped curve function with a rate maximum at ~pH 8. This is evident from the pseudo first-order rate constants given in table 3. The pK_as were evaluated as 6.27 ± 0.10 and 9.54 ± 0.14.

^{31}P NMR spectroscopy showed that at pH 10.5, the $[(NH_3)_5Co(bnpp)]^{2+}$ complex hydrolyzed to yield products with signals at −11.5, 6.5 and 17 ppm. At higher pH only the species at −11.5 and 6.5 ppm were observed and the former was identified as that due to free bnpp by adding excess ligand. The signal at 17 ppm was assigned to the N,O-chelate phosphoramidate. The pH dependence of its chemical shift and its hydrolytic behavior correlated with those observed previously [7]. The chemical shift varied from 17 to 31 ppm depending on the hydroxide ion concentration, attributed to deprotonation of the bridging nitrogen center. Hydrolysis of the chelate yielded N-bound monodentate phosphoramidate (6.5 ppm). This signal is near that for $[(NH_3)_5Co(npp)]^+$, a possible hydrolysis product arising from intermolecular attack by OH^- on the diester or from P–N bond cleavage in the chelate. However, addition of authentic $[(NH_3)_5Co(npp)]^+$ showed different signals at 6.5 and 6.4 ppm. Therefore, the signal at 6.5 ppm can be attributed to N-bound monodentate phosphoramidate.

3.2 cis*[(en)$_2$Co(OH$_2$)(OP(O)(OC$_6$H$_4$NO$_2$)$_2$)]S$_2$O$_6$ · H$_2$O*

cis$[(en)_2Co(OH_2)(bnpp)](S_2O_6)$, synthesized by reacting *cis*$[(en)_2Co(CF_3SO_3)_2]$ (CF_3SO_3) with an equivalent of bis(4-nitrophenyl)phosphate ion, was purified and then characterized by elemental analysis, ^{31}P and ^{1}H NMR spectrometry and UV/vis spectroscopy. The ^{31}P NMR chemical shift observed was that expected for bnpp coordinated to a Co(III) center in a monodentate mode [16–20]. Only one signal was

Table 4. Rate constant *vs.* pH for the initial step in the hydrolysis of *cis*$[(en)_2Co(OH_2)bnpp]^{2+}$.*

pH	Buffer	k_{obs} (s^{-1})
5.30	Acetate	0.0040 (±0.0002)
6.05	MES	0.023 (±0.001)
6.30	MES	0.034 (±0.001)
6.53	PIPES	0.061 (±0.002)
7.10	HEPES	0.114 (±0.006)
7.56	HEPES	0.150 (±0.006)
8.20	TRIS	0.170 (±0.009)
8.70	CHES	0.172 (±0.009)
9.00	CHES	0.175 (±0.009)
9.85	CAPS	0.187 (±0.006)
10.14	CAPS	0.181 (±0.006)

*Determined spectrophotometrically at 400 nm, $T = 25°C$, $I = 1.0$ M (NaCl).

observed, consistent with the product being either *cis* or *trans*. However, its reactivity was consistent only with it being the *cis* isomer.

Hydrolysis of the complex was followed by both UV/vis and ^{31}P NMR methods. Two consecutive nitrophenolate ion-releasing steps were clearly evident from the spectrophotometric study. Presumably, the first step defines the hydrolysis of the starting complex while the second step represents the subsequent hydrolysis of the product(s) from the first step. The pH dependence of the rate constants for the initial reaction is given in table 4.

The hydrolysis of the complex in the pH range 5–11 follows a rate law of the form:

$$k_{obs} = K_a k_m/(K_a + [H^+])$$

where k_m is the rate constant for the reaction of the deprotonated complex and K_a is the dissociation constant of the coordinated water molecule. The data in table 4 were fitted by a nonlinear least-squares program to obtain the values of these constants: $k_m = 0.18$ (±0.02) s^{-1}, $K_a = 1.37$ (±0.08) $\times 10^{-7}$ M^{-1} ($pK_a = 6.86$). The pK_a of the bound water was similar to that of the analogous Ir(III) complex [9] and about that expected for a dicationic Co(III) aqua amine species [21].

At high pH, the rate increased further. The observed kinetics over the whole pH range followed the rate law: $k_{obs} = K_a k_{m/}(K_a + [H^+]) + k_1\,[OH^-] + k_2\,[OH^-]^2$. The values for k_1 and k_2, 13.31 (±0.02) $dm^3\,mol^{-1}\,s^{-1}$ and 7.19 (±0.02) $dm^6\,mol^{-2}\,s^{-1}$, respectively, were obtained by nonlinear least-squares fitting of the data in table 5.

The phosphate species generated on hydrolysis of *cis*$[(en)_2Co(OH_2)(bnpp)]^{2+}$ were identified by ^{31}P NMR spectroscopy. At pH 5.20, the reactant (−5.9 ppm) decayed to a product at 6.7 ppm, with the same chemical shift as authentic *cis*$[(en)_2Co(OH_2)(npp)]^{2+}$ added as a marker. In the pH range 6–12, the disappearance of the reactant was too rapid to monitor by this method and the reaction observed was presumed to be the hydrolysis of the "intermediate" *cis*$[(en)_2Co(OH_2)(npp)]^{+}$. The hydrolysis components were identical to those found in a previous study [2] of *cis*$[(en)_2Co(OH_2)(npp)]^{+}$ under similar conditions: *cis* and *trans*$[(en)_2Co(OH_2)(npp)]^{+}$ (6.5 and 6.2 ppm, respectively), npp (−0.4 ppm), and the chelate $[(en)_2Co(O_2PO_2)]$ (24 ppm), or at higher pH, its ring-opened forms *cis* and *trans*$[(en)_2Co(OH)(OPO_3)]^{-}$ (13.7 and 13.5 ppm,

Table 5. Rate constants for the initial step in the hydrolysis of *cis*[(en)$_2$Co(OH$_2$)bnpp]$^{2+}$ at high pH.*

[OH$^-$]	k_{obs} (s^{-1})
0.05	0.77 (±0.01)
0.10	1.41 (±0.01)
0.25	3.78 (±0.04)
0.50	8.5 (±0.1)
0.75	13.9 (±0.1)
1.00	20.5 (±0.2)

*Determined spectrophotometrically at 400 nm, $T = 25^{\circ}$C, $I = 1.0$ M (NaCl).

respectively). In addition, 14–35% free unreacted bnpp (−11.8 ppm) was produced as the base concentration was increased. The UV/vis kinetic data of the "intermediate" were also close to those obtained with authentic *cis*[(en)$_2$Co(OH$_2$)(npp)]$^+$ [2].

4. Discussion

4.1 *Mechanism of hydrolysis of [(NH$_3$)$_5$Co(bnpp)]$^{2+}$*

Based on previous studies of related systems [6–9], the most likely route for the hydrolysis of the first nitrophenolate group in [(NH$_3$)$_5$Co(bnpp)]$^{2+}$ is via attack of a bound amido ion at the phosphorus center of the diester complex (scheme 1). This arises from deprotonation of a *cis* ammonia ligand in basic media. The N,O chelate phosphoramidate monoester **3** would be the initial product of such a reaction after decay of the aminophosphorane diester intermediate **1**. This pathway accounts for 67% of the reactant. The remaining 33% is accommodated by conjugate base dissociation of the phosphate diester via Co–O bond rupture (scheme 1, path b), a not uncommon feature of such Co(III) ammine complex reactivity [22,23].

By analogy with previous phosphate chemistry [5], the aminophosphorane **1** is depicted as a five-coordinate intermediate or activated complex with a trigonal bipyramidal geometry. This path is either concerted or intermediate **1** is very short lived as no exchange with solvent H$_2$O has been observed with the npp complex [6]. By implication, *pseudo*-rotation is also unlikely and apical entry of the amido nucleophile and departure of a nitrophenol(-ate) from the other apical position is likely to prevail. The four-membered chelate ring in the aminophosphorane would be required to span apical–equatorial positions [5] in the trigonal bipyramidal intermediate or activated complex **1** to minimize strain. Therefore, the most likely structure for the aminophosphorane is that with an apical nitrogen and a *trans* apical nitrophenol group placed ready for expulsion. The failure to observe an aminophosphorane intermediate cannot be used to make an unambiguous choice between a concerted and a nonconcerted process. It could merely reflect a short lifetime for the intermediate. In addition, the observed kinetics do not distinguish between the two pathways. The first-order dependence of rate on [OH]$^-$ is consistent with either process, so the issue of concertedness or intermediacy is still unresolved and an even better leaving group than that used here would be required to sense the intermediate if it exists.

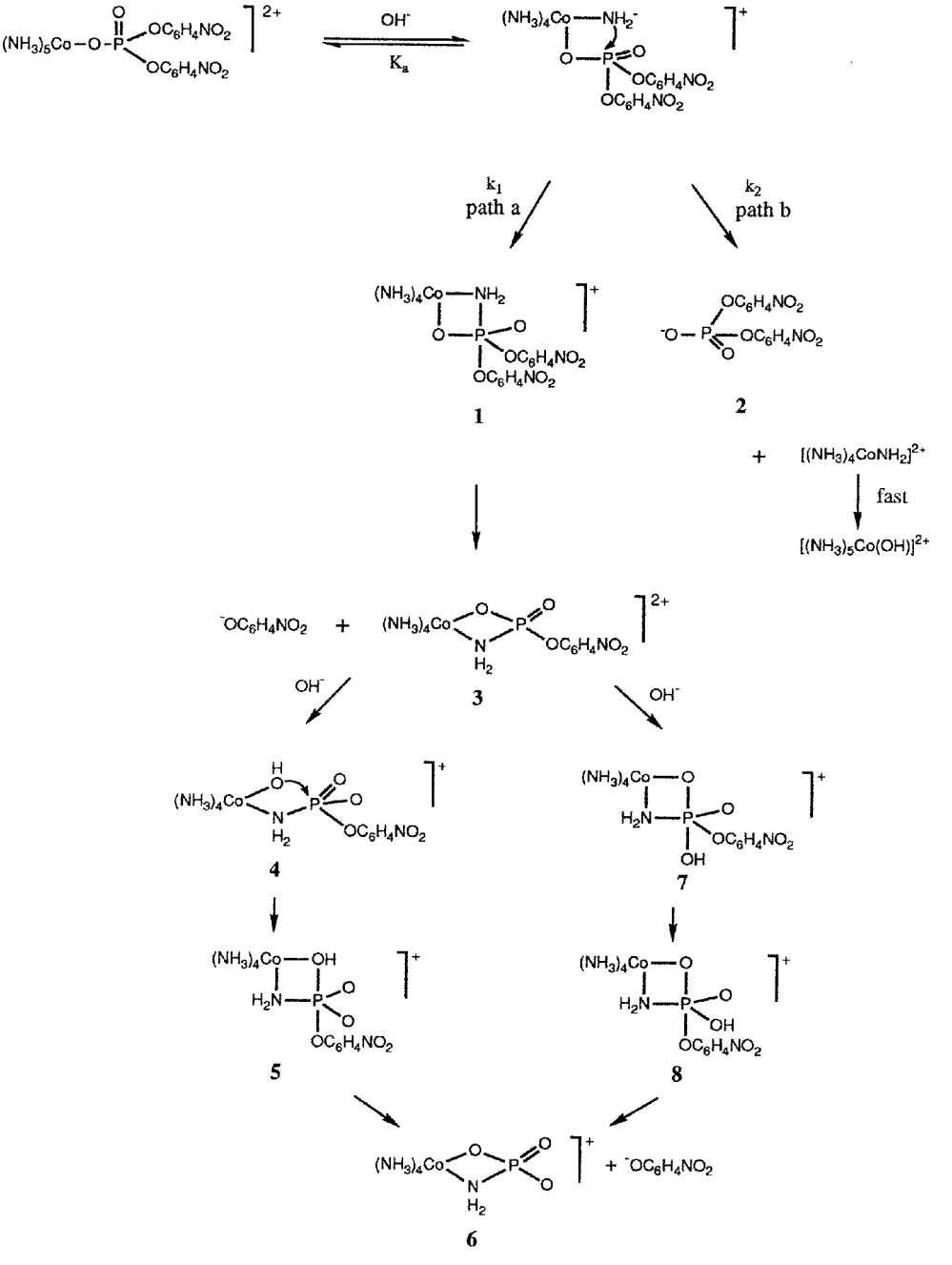

Scheme 1. Pathways for coordinated amido ion reacting with the phosphate diester.

Hydrolysis of the nitrophenolate group in **3** to give the N,O chelate phosphoramidate **6** proceeded in 97% yield. This step follows a bell-shaped pH–rate constant profile (table 3), which can be attributed to two deprotonated intermediates. Given the likely pathway for the initial step, the final N,O chelate phosphoramidate **6** could arise from

two possible processes: by rapid ring opening of **3** to give **4**, followed by intramolecular attack of Co–OH^- at coordinated npp, or by rapid intermolecular hydrolysis of the N,O chelate phosphoramidate monoester **3** by OH^-.

The release of nitrophenolate ion from **3** could occur by a similar mechanism to that of cyclic organic phosphate esters. In this process, exocyclic P–O bond cleavage takes place and the ring structure is retained. The aminophosphorane **7**, generated initially by apical attack of OH^- at the phosphorus center of **3**, would need to undergo *pseudo*-rotation to expel the now apical nitrophenolate group of **8**. However, such *pseudo*-rotations have yet to be established in metal ion–phosphate systems.

Ring opening is a more likely path, via an S_N1(CB) Co–O bond rupture [2,6–8], by analogy with related Co(III) systems. To date, P–O rupture has not been observed in preference to such Co–O ruptures. Hydrolysis of the nitrophenolate group in **4** could then proceed via efficient intramolecular attack of Co–OH^- at the phosphorus center and the aminophosphorane **5** thus formed would decay to the N,O chelate phosphoramidate product **6**. The pH–rate constant profile observed for this step is consistent with a reaction involving **4**, but not with a reaction involving **7**. Two deprotonations appear to be involved. The increase in k_{obs} for the pH range 5–8 is ascribed to deprotonation of the aqua ligand (pK_a 6.27 ± 0.10) to give the Co–OH nucleophile. The subsequent reduction in k_{obs} on further raising the pH is attributed to deprotonation of the phosphoramidate nitrogen (pK_a 9.54 ± 0.14). The deprotonation effectively reduces the electrophilic character of the phosphorus atom and diminishes its ability to accept a nucleophile. These assignments are supported by analogous Ir(III) chemistry [9], where the reactive intermediate, equivalent to **4**, was observed by ^{31}P NMR spectroscopy. The kinetics of hydrolysis of this system also followed a bell-shaped pH–rate constant profile, with pK_a values of 6.39 ± 0.02 and 9.76 ± 0.05, respectively. So the parallel between the two systems is clear.

4.2 *Base hydrolysis of* cis*[(en)$_2$Co(OH$_2$)(bnpp)]$^{2+}$*

A mechanism that accommodates (1) the sigmoidal dependence of the rate on pH (in the pH range 5–14), (2) the essentially pH-independent region of the rate profile (pH 8–11), (3) the production of *cis*-$[(en)_2Co(OH_2)(npp)]^+$ and some free bnpp in the pH range 5–12 and (4) the large rate enhancement relative to the uncoordinated ester in the base hydrolysis of *cis*-$[(en)_2Co(OH_2)(bnpp)]^{2+}$ in the pH range 5–11 is given in scheme 2. Thus, at pH < 11, formation of *cis*-$[(en)_2Co(OH)(npp)]$ presumably occurs via an intramolecular nucleophilic reaction of the Co–OH ion at the phosphorus center. The pH 5–8 dependence of the initial rate is attributed to deprotonation of the coordinated water ligand to generate the reactive hydroxo species. The rate of the intramolecular reaction levels out at ~pH 8.5 ($k_m = 0.18 \pm 0.02\ s^{-1}$) and remains independent of pH in the range 8.5–11 as expected for the deprotonated nucleophile Co–OH.

The phosphorane intermediate **11**, formed initially, decays to yield the chelate phosphate monoester **12**, which then rapidly ring opens, almost certainly via Co–O bond rupture to produce **13** (scheme 2, path a). Although tracer experiments have not been performed in this instance, in related cases where they have been carried out the ring always opens via Co–O bond cleavage [2,6]. However, the same situation is not evident for the Ir(III) analogs [9], where it appears to be simply a function of the relative P–O and M–O bond reactivities. The logical route, therefore, for the loss of unreacted bnpp is via the conjugate base dissociative path (scheme 2, path b)

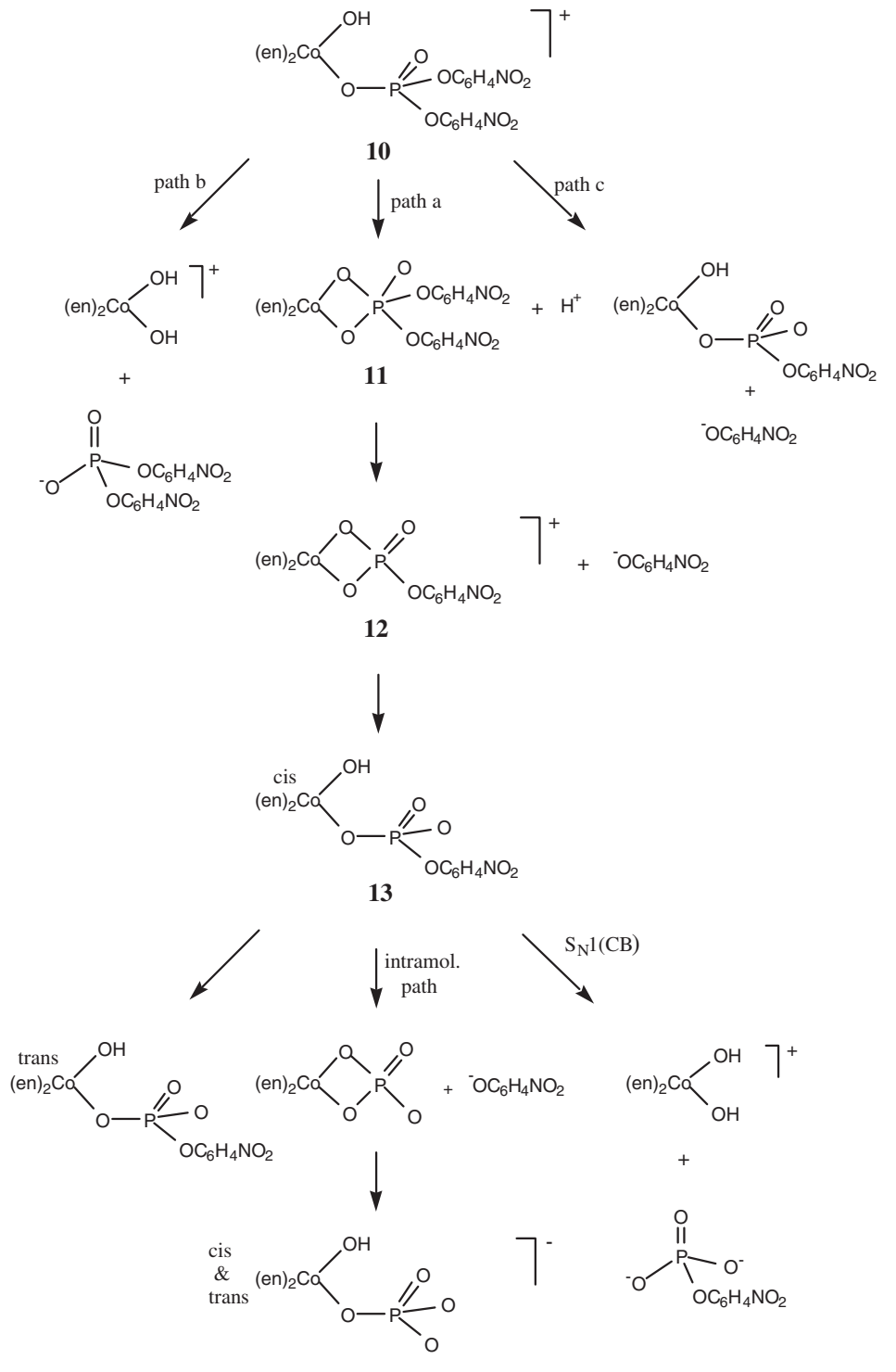

Scheme 2. Pathways for the coordinated hydroxide ion reacting with phosphate diester.

characteristic of Co(III) amine chemistry [22,23]. This reaction is not relevant to the main thrust of this study and is therefore not considered further.

Above the pH-independent plateau there is a further increase in the rate of ester hydrolysis (scheme 2, path c). It is therefore apparent that another mechanism for nitrophenolate release arises in this region and there are several possibilities that would account for such a result and still yield *cis*[$(en)_2$Co(OH)(npp)]. They include, first, an intermolecular attack of hydroxide ion at the phosphorus center where the products of such a reaction would be identical to those observed from the intramolecular path. However, in general, there is no sign of such intermolecular additions of OH^- at phosphorus centers of phosphate diesters bound to metal centers [9], so this path appears unlikely. Second, deprotonation of the coordinated hydroxide ($pK_a \sim 20$) [24] could take place to allow intramolecular attack by coordinated oxide ion. A similar mechanism has been proposed for base-catalyzed intramolecular reactions of coordinated olefins adjacent to a bound hydroxide ion [25]. In order to produce a significant increase in the rate at pH 14, $Co–O^-$ would need to be at least 10^6 times more effective as an intramolecular nucleophile than $Co–OH^-$. The difference in pK_a values of the two nucleophiles ($\sim 10^{13}$) could account for a difference of this magnitude. Thus, attack by Co–O could make a significant contribution to the rate at pH 14, even though only $\sim 10^{-4}$% of Co–OH would be deprotonated. The third possibility is a rate-limiting decomposition of a phosphorane intermediate formed by intermolecular attack of hydroxide at the phosphorus center of the diester complex and deprotonation by the bound hydroxide ion. Such a pathway has not been detected by the tracer experiments in related cases and the intramolecular nucleophile has always been more efficient; therefore it appears unlikely. Finally, an intermolecular attack of hydroxide ion at the phosphorus center of the oxyphosphorane might take place to give a six-coordinate intermediate or activated complex. There is considerable evidence for the participation of hexacoordinated phosphorus species in the base-catalyzed hydrolyses of alkoxy ligands on oxyphosphoranes [26–28]. This type of mechanism has also been used to account for the incorporation of ^{18}O label ($\sim$20%) into the exocyclic oxygen atoms of the chelate product derived from the reaction of unlabeled *cis*[$(en)_2$Co(OH)(npp)] in labeled water (pH 10) [2]. In this example, water is the active species in the intermolecular attack at the phosphorane, but at higher pH, decomposition of the pentaoxyphosphorane by the intervention of a hydroxide ion in the activated complex could be envisaged. An analogous pathway could also occur with the *cis*[$(en)_2$Co(OH)(bnpp)]$^+$ complex, but with the available data it is not possible to distinguish between these mechanisms.

The hydrolytic behavior of *cis*[$(en)_2$Co(OH)(npp)] has also been extensively studied [2] and parallels that observed for the intermediate in the hydrolysis of cis[$(en)_2$Co(OH)(bnpp)]$^+$. The pathways involved in its decomposition are summarized in the latter part of scheme 2.

To help understand the factors that govern this chemistry in general, it is instructive to draw some comparisons between the data here and those of related studies.

4.3 *Free ligand* vs. *complexed ligand for* $[(NH_3)_5Co(OP(O)(OC_6H_4NO_2)_2)](CF_3SO_3)_2$

Hydrolysis of the free ligand bnpp [29] obeys a rate law that is first order in hydroxide and has an overall second-order rate constant of $(1.3 \pm 0.1) \times 10^{-5}\,dm^3\,mol^{-1}\,s^{-1}$ at 25°C,

$\mu = 1.0$ M. The release of nitrophenolate ion is enhanced $\sim 10^6$-fold on coordination to the $(NH_3)_5Co-$ moiety and the evaluation of the enhancement increases when the effective concentration of the intramolecular nucleophile is taken into consideration. Thus, a conservative estimate of the rate enhancement, allowing for the proportion of the active nucleophile present, is $\sim 10^8$. This yields a first-order rate constant of $\sim 10^3\ s^{-1}$ for attack of the amido ion on the phosphorus center and elimination of the phenol. Such a rate constant approaches those of enzymic systems.

4.4 *Cobalt* vs. *iridium*

In 1 M NaOH, ester cleavage for $[(NH_3)_5Co(bnpp)]^{2+}$ is $\sim 10^3$ times faster than that for the analogous Ir(III) species and rate differences of this magnitude have been observed for related Co(III)/Ir(III) systems [9]. The slower rate for the Ir(III) systems can be attributed to increased strain in forming the 4-chelate with the larger Ir(III) ion [30] (vide infra). The difference in pK_a between the two species ($\sim$16 and 17 for ammonia coordinated to Co(III) and Ir(III), respectively [31,32]) does not account for the rate variation [30] of the amido nucleophile either on a basicity or a concentration basis.

A more direct comparison and a similar difference was evident for the reactivity of $[(NH_3)_4Co(OH)NH_2P(O)(OC_6H_4NO_2)_2]$ *vs.* $[(NH_3)_4Ir(OH)NH_2P(O)(OC_6H_4NO_2)_2]$. At pH 8, 25°C, the rate constants for intramolecular attack of OH at the phosphorus center in the Co(III) and Ir(III) [9] complexes are $1.3\ s^{-1}$ and $3.1 \times 10^{-3}\ s^{-1}$, respectively, and presumably for much the same reason as that described above.

Under similar conditions, *cis*$[(en)_2Co(OH_2)(bnpp)]^{2+}$ and *cis*$[(en)_2Co(OH_2)(npp)]^{+}$ are also hydrolyzed $\sim 10^3$ times faster than the analogous Ir(III) species [33]. The differences in reactivity can be attributed to the different sizes of the two metal ions [34] (effective ionic radii for Co(III) and Ir(III) are 0.545 and 0.68 Å, respectively [35]), which influences the relative strain induced in forming the four-membered ring in the intramolecular reaction (Ir > Co) [1]. This effect also accounts for the failure to observe such Ir(III) 4-chelates. By contrast, the tris-bidentate $[(en)_2Co(O_2PO_2)]$ species [1] is the thermodynamically preferred form of the phosphate complex in the pH range 6–9 [36]. Such effects are inevitably reflected in the variation of the rate constants observed for the Co(III) *versus* Ir(III) complexes and the general chemistry involved.

4.5 *Monoester* vs. *diester*

The rate of *cis* bound amido ion attack at the phosphorus center of $[(NH_3)_5\,Co(bnpp)]^{2+}$ is $\sim$350 times faster than for the analogous monoester complex. This difference in reactivity presumably also reflects the inherent electrophilic character of the phosphorus atoms in these systems and it seems more appropriate to view them as *pseudo* diesters and triesters while they are coordinated to the metal ion. Certainly, there is no sign of a metaphosphate pathway with the coordinated monoester.

Overall, the chelated amido phosphate monoester complex was not observed despite the increase in reactivity arising from coordination of the diester to the Co(III) ion and the enhanced capability of the leaving group. It seems likely that even if better leaving groups are installed, that chelate would still prefer to react by Co–O bond rupture rather than by *pseudo*-rotation and exocyclic hydrolysis of the ester group. One effect influences the other.

4.6 *Comparisons with phosphate ester hydrolysis by other* cis- *tetraamineCo(III) complexes*

Chin and Zou obtained a rate constant of $2.7 \times 10^{-5}\,s^{-1}$ at pH 7, 50°C, for the *cis*$[(en)_2Co(OH)(OH_2)]^{2+}$-promoted hydrolysis of bnpp [10], dramatically less than the rate for the preformed bnpp complex ($0.15\,s^{-1}$) described here even at 25°C. This hydrolysis is so slow that it must be even more than substitution of the phosphate ester that is limiting the hydrolysis ($< k(H_2Oex) = 4.7 \times 10^{-4}\,s^{-1}$, 25°C) [37]. Possibly the *trans* isomer is formed preferentially in the initial anation step and has to rearrange to the *cis* form before appreciable hydrolysis can occur.

The following examples also appear to illustrate the significance of the anation in such overall ester hydrolyses.

The rate constants for the release of nitrophenolate ion from *cis*$[(en)_2Co(OH_2)(npp)]^{+}$ and the complementary *cis*$[(en)_2Co(OH)(OH_2)]^{2+}$/npp system are $2.15 \times 10^{-4}\,s^{-1}$ (pH 7, 25°C) and $3.0 \times 10^{-4}\,s^{-1}$ (pH 7, 50°C), respectively [10]. The rate constant at 25°C for the latter system is estimated as $\sim 10^{-5}\,s^{-1}$, using a reasonable $\Delta H^{\neq}$ value of $24\,kcal\,mol^{-1}$. The two systems must have different rate-determining steps. With the prebound ester the rate-limiting step is intramolecular attack of bound OH^- at the phosphorus center while in the other, anation is clearly one limiting step and may be *trans cis* rearrangement also.

At pH 7, 25°C, *cis*$[(en)_2Co(OH_2)(bnpp)]^{2+}$ hydrolyzes ~600 times faster than the monoester complex *cis*$[(en)_2Co(OH_2)(npp)]^{+}$. Under similar conditions the *cis*$[(en)_2Co(OH)(OH_2)]^{2+}$-promoted hydrolysis of the diester is slower (~10-fold) than that of the monoester (table 6). The hydrolysis rates observed with the preformed complexes reflect directly the rates of intramolecular attack of OH^- at the phosphorus. By contrast, the *cis*$[(en)_2Co(OH)(OH_2)]^{2+}$-promoted hydrolysis of mono- and diester phosphates are clearly contrary to this conclusion and must therefore reflect rate-limiting steps elsewhere in the process.

The pattern of reactivity is not always so variable. For example, the *cis*$[(trpn)Co(OH)(OH_2)]^{2+}$-promoted rate of hydrolysis of the dnpp monoester is only slightly greater than that of the diester bdnpp (~5-fold) [11]. This largely reflects the rapid substitution for the trpn reagent. Such rapid rates for anation and axiomatically dissociation of the substrates provide more effective reagents. However, they also inhibit detailed analysis of the processes. A more detailed comparison of such reagents in polyphosphate cleavage has been documented elsewhere [38].

The rate constant ($0.17\,s^{-1}$) for the hydrolysis of *cis*$[(en)_2Co(OH_2)(bnpp)]^{2+}$ at pH 8, 25°C, yields a rate enhancement of $\sim 10^8$ over that of the free ligand under the same

Table 6. Rate constants for hydrolysis reactions involving Co(III) complexes of bnpp and npp.

System	k (s^{-1})	Reaction conditions
cis$[(en)_2Co(OH_2)bnpp]^{2+}$	0.114	pH 7.10, 25°C
cis$[(en)_2Co(OH_2)npp]^{+}$	2.15×10^{-4}	pH 7.10, 25°C
	2.0×10^{-4}	pH 7.10, 25°C
bnpp/*cis*$[(en)_2Co(OH)(OH_2)]^{2+}$	2.7×10^{-5}	pH 7.0, 50°C (10)
	$\sim 10^{-6}$ *	pH 7.0, 25°C
npp/*cis*$[(en)_2Co(OH)(OH_2)]^{2+}$	3.0×10^{-4}	pH 7.0, 50°C (10)
	$\sim 10^{-5}$ *	pH 7.0, 25°C

*Rate constants estimated using $\Delta H^{\neq} = 24\,kcal\,mol^{-1}$.

conditions. Similar enhancements have also been observed in other *cis*[(N_4)Co(OH)(OH_2)]$^{2+}$ [N_4 = trpn, cyclen (= 1,4,7,10-tetraaza-cyclododecane)] promoted hydrolyses of a series of diesters [39]. By comparison, metal ion-promoted hydrolyses of monoesters give only 10^5–10^6 rate enhancements. This is a curious observation as the uncoordinated monoesters, in general, hydrolyze more rapidly than the diesters at neutral pH, ascribed to a metaphosphate pathway [40]. The rate enhancements are less ($\sim 10^2$) for the Co(III) complex-promoted hydrolysis of monoesters with inferior leaving groups such as methyl phosphate [3] but it is also quite clear that the coordinated nitrophenyl monoester is reacting with the intramolecular nucleophile and not hydrolysing by a metaphosphate path. The chelated intermediate phosphorane is evident from ^{18}O tracer experiments and the product is chelated phosphate ion [2]. In this respect the coordinated monoester is behaving more like a diester and the coordinated diester presumably mimics triester chemistry to a degree. This character may obviate the metaphosphate pathway.

Although even more reactive [(N_4)Co(OH)(OH_2)]$^{2+}$ systems are required for the efficient cleavage of less activated phosphate diesters, such as the backbone of nucleic acids, these simple studies help to identify features that can enhance reactivity in such processes. Clearly, anation should not be a rate-limiting step to get efficiency with such reagents and although there does seem to be some influence of the type of Co(III)-bound tetraamine ligand on the rate of intramolecular attack, at present it is not large.

Finally, large enhancements in the rates of hydrolysis and aminolysis do arise from coordination of the ester moiety and the adjacent intramolecular nucleophiles. The rates even approach those observed in enzymic systems if allowance is made for the concentration of the coordinated nucleophile. The complexes also display facile phosphoryl group transfers from oxygen to nitrogen using the metal ion as a template to hold the pieces together. All of this enhances our understanding of the roles for metal ions in such reactions. That should be relevant to the metal-containing biological systems and the design of catalysts for phosphate-ester hydrolysis, phosphoryl transfer and polyphosphate degradation.

Acknowledgments

We are grateful for microanalyses from the ANU Analytical Section and an ANU Scholarship for R.W.

References

[1] B. Anderson, R.M. Milburn, J.N. Harrowfield, G.B. Robertson, A.M. Sargeson. *J. Am. Chem. Soc.* **99**, 2652 (1977).
[2] D.R. Jones, L.F. Lindoy, A.M. Sargeson. *J. Am. Chem. Soc.* **105**, 7327 (1983).
[3] F.J. Farrel, W.A. Kjellstrom, T.G. Spiro. *Science* **164**, 320 (1969).
[4] J. Kumamoto, J.R. Cox, F.H. Westheimer. *J. Am. Chem. Soc.* **78**, 4858 (1956).
[5] F.H. Westheimer. *Acc. Chem. Res.* **1**, 70 (1968).
[6] J.N. Harrowfield, D.R. Jones, L.F. Lindoy, A.M. Sargeson. *J. Am. Chem. Soc.* **102**, 7733 (1980).
[7] P. Hendry, A.M. Sargeson. *Inorg. Chem.* **25**, 865 (1986).
[8] I.I. Creaser, R.V. Dubs, A.M. Sargeson. *Aust. J. Chem.* **37**, 1999 (1984).
[9] P. Hendry, A.M. Sargeson. *Inorg. Chem.* **29**, 97 (1990).
[10] J. Chin, X. Zou. *J. Am. Chem. Soc.* **110**, 223 (1988).

[11] G. Rawji, M. Hediger, R.M. Milburn. *Inorg. Chim. Acta* **79**, 247 (1983).
[12] N.E. Dixon, W.G. Jackson, M.J. Lancaster, G.A. Lawrance, A.M. Sargeson. *Inorg. Chem.* **20**, 470 (1981).
[13] N.E. Dixon, W.G. Jackson, G.A. Lawrance, A.M. Sargeson. *Inorg. Synth.* **22**, 103 (1983).
[14] N.E. Dixon, G.A. Lawrance, P.A. Lay, A.M. Sargeson. *Inorg. Chem.* **23**, 2946 (1984).
[15] P.R. Bevington. *Data Reduction and Error Analysis for the Physical Sciences*, p. 92, McGraw-Hill, New York (1969).
[16] V.F. Seel, G. Bohnstedt. *Z. Anorg. Allg. Chem.* **435**, 257 (1977).
[17] R.D. Cornelius, P.A. Hart, W.W. Cleland. *Inorg. Chem.* **16**, 2799 (1977).
[18] I. Lin, W.B. Knight, S.-J. Ting, D. Dunaway-Mariano. *Inorg. Chem.* **23**, 988 (1984).
[19] P. Hendry, PhD thesis, Ch. 5, The Australian National University (1985).
[20] D.G. Gorenstein. *J. Am. Chem. Soc.* **97**, 898 (1975).
[21] D.A. Buckingham, C.E. Davis, A.M. Sargeson. *J. Am. Chem. Soc.* **92**, 6159 (1970).
[22] M.L. Tobe. *Acc. Chem. Res.* **3**, 377 (1970) and references therein.
[23] A.M. Sargeson. *Pure Appl. Chem.* **33**, 527 (1973).
[24] C. Boreham, D.A. Buckingham, F.R. Keene. *J. Am. Chem. Soc.* **101**, 1409 (1979).
[25] L.R. Gahan, J.N. Harrowfield, A.J. Herlt, L.F. Lindoy, P.O. Whimp, A.M. Sargeson. *J. Am. Chem. Soc.* **107**, 6231 (1985)
[26] P. Gillespie, F. Ramirez, I. Ugi, D. Marquarding. *Angew. Chem., Int. Ed. Engl.* **12**, 9 (1973).
[27] F. Ramirez, V.A.V. Prasad, J.F. Marecek. *J. Am. Chem. Soc.* **96**, 7269 (1974).
[28] F. Ramirez, H.J. Kugler, A.V. Patwardham, C.P. Smith. *J. Org. Chem.* **33**, 1185 (1968).
[29] P. Hendry, PhD thesis, p. 118, The Australian National University (1985).
[30] P. Hendry, PhD thesis, p. 120, The Australian National University (1985).
[31] J.W. Palmer, F.J. Basolo. *Inorg. Nucl. Chem.* **15**, 279 (1960).
[32] A. Zanella, P.C. Ford. *Inorg. Chem.* **14**, 700 (1975).
[33] P. Hendry, A.M. Sargeson. *J. Am. Chem. Soc.* **111**, 2521 (1989).
[34] P. Hendry, PhD thesis, p. 151, The Australian National University (1985).
[35] R.D. Shannon. *Acta Cryst.* **A32**, 751 (1976).
[36] S.F. Lincoln, D.R. Stranks. *Aust. J. Chem.*, **21**, 37, 57, 67, 1733 and 1745 (1968).
[37] W. Kruse, H. Taube. *J. Am. Chem. Soc.* **83**, 1280 (1961).
[38] R.J. Geue, A.M. Sargeson, R. Wijesekera. *Aust. J. Chem.* **46**, 1021 (1993).
[39] J. Chin, M. Banaszczyk, V. Jubian, X. Zou. *J. Am. Chem. Soc.* **111**, 186 (1989).
[40] J.P. Guthrie. *J. Am. Chem. Soc.* **99**, 3991 (1977).